JOC Article

Experimental and DFT Studies on Competitive Heterocyclic Rearrangements. Part 2:[1] A One-Atom Side-Chain versus the Classic Three-Atom Side-Chain (Boulton−Katritzky) Ring Rearrangement of 3-Acylamino-1,2,4-oxadiazoles‡

Andrea Pace,*,† Ivana Pibiri,† Antonio Palumbo Piccionello,† Silvestre Buscemi,† Nicolò Vivona,† and Giampaolo Barone*,§

Dipartimento di Chimica Organica "E. Paternò" and Dipartimento di Chimica Inorganica e Analitica "S. Cannizzaro", Università degli Studi di Palermo, Viale delle Scienze, Parco d'Orleans II, Edificio 17, I-90128 Palermo, Italy

pace@unipa.it; gbarone@unipa.it

Received June 19, 2007

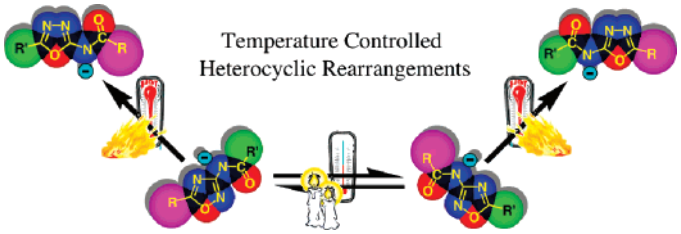

The experimental investigation of the base-catalyzed rearrangements of 3-acylamino-1,2,4-oxadiazoles evidenced a new reaction pathway which competes with the well-known ring-degenerate Boulton−Katritzky rearrangement (BKR). The new reaction consists of a one-atom side-chain rearrangement that is base-activated, occurs at a higher temperature than the BKR, and irreversibly leads to the corresponding 2-acylamino-1,3,4-oxadiazoles. An extensive DFT study is reported to elucidate the proposed reaction mechanism and to compare the three possible inherent routes: (i) the reversible three-atom side-chain ring-degenerate BKR, (ii) the ring contraction−ring expansion route (RCRE), and (iii) the one-atom side-chain rearrangement. The results of the computational investigation point out that the latter route is kinetically preferred over the RCRE and can be considered as the ground-state analogue of a previously proposed C(3)−N(2) migration−nucleophilic attack−cyclization (MNAC) photochemically activated pathway. The MNAC consists of the formation of a diazirine intermediate, involving the exocyclic nitrogen, that eventually evolves into a carbodiimide intermediate (migration); the latter undergoes a single intramolecular nucleophilic attack−cyclization step leading to the final 2-acylamino-1,3,4-oxadiazole.

Introduction

Heterocyclic ring rearrangements represent a class of reactions which is largely documented in the literature.[2] In the hands of the synthetic heterocyclist, these rearrangements are a useful tool in order to obtain different heterocyclic systems. Moreover, these reactions are very important to assess both the thermal and photochemical stability of heterocyclic systems that are widely used as biologically active molecules, pharmaceuticals, and new materials in thermally and/or (photo)electronically stressed devices.[3]

Among the most investigated ring-transformation reactions, the monocyclic Boulton−Katritzky rearrangement (BKR) con-

‡ Dedicated to Professor Domenico Spinelli in the occasion of his 75th birthday.

† Dipartimento di Chimica Organica "E. Paternò". Fax: +39091596825.

§ Dipartimento di Chimica Inorganica e Analitica "S. Cannizzaro". Fax: +39091427584.

(1) For Part 1, see: Pace, A.; Buscemi, S.; Vivona, N.; Silvestri, A.; Barone, G. *J. Org. Chem.* **2006**, *71*, 2740−2749.

(2) See for example: (a) Van der Plas, H. C. *Ring Transformation of Heterocycles*; Academic Press: New York, 1973; Vol. 1. (b) Van der Plas, H. C. *Ring Transformation of Heterocycles*; Academic Press: New York, 1973; Vol. 2. (c) L'abbè, G. *J. Heterocycl. Chem.* **1984**, *21*, 627−638. (d) Van der Plas, H. C. *Adv. Heterocycl. Chem.* **1999**, *74*, 1−253. See also specific classes of ring transformations reviewed in: (e) *Comprehensive Heterocyclic Chemistry*; Katritzky, A. R., Rees, C. W., Eds; Pergamon Press: Oxford, 1984; Vols. 1−8. (f) *Comprehensive Heterocyclic Chemistry II*; Katritzky, A. R., Rees, C. W., Scriven, E. F. V., Eds; Elsevier: Amsterdam, 1996; Vols. 1−9.

10.1021/jo701306t CCC: $37.00
Published on Web 09/07/2007

SCHEME 1. General Scheme of the Boulton−Katritzky Rearrangement (BKR)

1 **2**

sists of an interconversion between two five-membered heterocycles where a three-atom side chain and a pivotal annular nitrogen are involved (Scheme 1).[4] This reaction is widely documented in the literature because of its application in the synthesis of several target molecules[2c,4,5] as well as for the intriguing mechanistic aspects.[6] This reaction, also classified as an internal nucleophilic substitution,[5a,b,6a−f,7] typically occurs on 1-oxa-2-azoles (**1**; D = O) that are O−N bond-containing five-membered heterocycles [isoxazoles,[5a,b] 1,2,4-oxadiazoles,[5] 1,2,5-oxadiazoles (furazans),[5a,b] and 1,2,5-oxadiazole-2-oxides (furoxans)[5a,b,8]].

When the nucleophilic Z atom in the side chain attacks the electrophilic N(2) ring nitrogen, the O(1) ring oxygen in (**1**; D = O) acts as an internal leaving group and the O−N bond is cleaved. When the Z atom is different from oxygen (for instance, Z = N, S, C), the process is irreversible, the driving force being the formation of a more stable N−N, S−N, or C−N bond replacing the less stable O−N bond. In this case, the reactivity toward the BKR will be determined by the structure of the starting heterocycle, the nucleophilic character of the Z atom, the nature of the solvent, and the possible presence of a base.[9] On the other hand, when Z is also an oxygen atom (**1**; D = Z = O), the reaction is potentially reversible since an O−N bond is broken and a new one is formed. In such a case, other factors

SCHEME 2

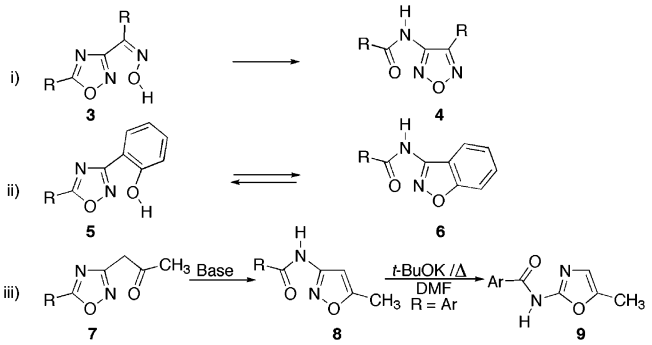

3 **4** **5** **6** **7** **8** **9**

(the intrinsic ring stability, the nature and position of the substituents, etc.) become important in determining the direction of the equilibrium and, in some cases, the irreversibility of the reaction. Some typical rearrangements of this kind, referred to the 1,2,4-oxadiazole ring as a substrate, are (Scheme 2) (i) the stereospecific spontaneous irreversible transformation of *Z*-oximes of 3-acyl-1,2,4-oxadiazoles **3** into the corresponding 3-acylamino-1,2,5-oxadiazoles (furazans) **4**;[10,11] (ii) the base-catalyzed interconversion between 3-(*o*-hydroxyphenyl)-1,2,4-oxadiazoles **5** and 3-acylamino-benzisoxazoles **6**, where the equilibrium composition depends on factors such as the type of base used (strong bases favoring the oxadiazole) and the nature of the R substituent;[12] and (iii) the irreversible base-catalyzed rearrangement of the enolate form of 3-acetonyl-1,2,4-oxadiazoles **7** into the corresponding 3-acylaminoisoxazoles **8**.[13] In turn, the rearrangement of isoxazole (**8**; R = Ar) into oxazole **9** has been reported by heating in DMF in the presence of *t*-BuOK and was suggested to occur through a ring contraction−ring expansion (RCRE) mechanism involving a deprotonated form of the starting acylaminoisoxazole **8**.[14]

(3) (a) Pozharskii, A. F.; Soldatenkov, A. T.; Katritzky, A. R. *Heterocycles in Life and Society*; Wiley: Chichester, UK, 1997. (b) *Comprehensive Heterocyclic Chemistry*; Katritzky, A. R., Rees, C. W., Eds; Pergamon Press: Oxford, 1984; Vol. 1.

(4) (a) Boulton, A. J.; Katritzky, A. R.; Hamid, A. M. *J. Chem. Soc. (C)* **1967**, 2005−2007. (b) Afridi, A. S.; Katritzky, A. R.; Ramsden, C. A. *J. Chem. Soc., Perkin Trans. 1* **1976**, 315−320.

(5) (a) Ruccia, M.; Vivona, N.; Spinelli, D. *Adv. Heterocycl. Chem.* **1981**, *29*, 141−169. (b) Vivona, N.; Buscemi, S.; Frenna, V.; Cusmano, G. *Adv. Heterocycl. Chem.* **1993**, *56*, 49−154. (c) Korbonits, D.; Kanzel-Szvoboda, I.; Horváth, K. *J. Chem. Soc., Perkin Trans. 1* **1982**, 759−766. (d) Horváth, K.; Korbonits, D.; Naráy-Szabò, G.; Simon, K. *J. Mol. Struct. (THEOCHEM)* **1986**, *136*, 215−227.

(6) For recent mechanistic studies on azole-to-azole interconversion reactions of the Boulton−Katritzky type, see: (a) Cosimelli, B.; Guernelli, S.; Spinelli, D.; Buscemi, S.; Frenna, V.; Macaluso, G. *J. Org. Chem.* **2001**, *66*, 6124−6129. (b) Cosimelli, B.; Frenna, V.; Guernelli, S.; Lanza, C. Z.; Macaluso, G.; Petrillo, G.; Spinelli, D. *J. Org. Chem.* **2002**, *67*, 8010−8018. (c) D'Anna, F.; Frenna, V.; Macaluso, G.; Morganti, S.; Nitti, P.; Pace, V.; Spinelli, D.; Spisani, R. *J. Org. Chem.* **2004**, *69*, 8718−8722. (d) D'Anna, F.; Ferroni, F.; Frenna, V.; Guernelli, S.; Lanza, C. Z.; Macaluso, G.; Pace, V.; Petrillo, G.; Spinelli, D.; Spisani, R. *Tetrahedron* **2005**, *61*, 167−178. (e) D'Anna, F.; Frenna, V.; Macaluso, G.; Marullo, S.; Morganti, S.; Pace, V.; Spinelli, D.; Spisani, R.; Tavani, C. *J. Org. Chem.* **2006**, *71*, 5616−5624. For DFT studies on monocyclic BKR, see: (f) Bottoni, A.; Frenna, V.; Lanza, C. Z.; Macaluso, G.; Spinelli, D. *J. Phys. Chem. A* **2004**, *108*, 1731−1740. Moreover, for DFT studies on bicyclic BKR, see for example: (g) Eckert, F.; Rauhut, G. *J. Am. Chem. Soc.* **1998**, *120*, 13478−13484. (h) Rauhut, G. *J. Org. Chem.* **2001**, *66*, 5444−5448. (i) Peña-Gallego, A.; Rodríguez-Otero, J.; Cabaleiro-Lago, E. M. *J. Org. Chem.* **2004**, *69*, 7013−7017.

(7) Vivona, N.; Cusmano, G.; Ruccia, M.; Spinelli, D. *J. Heterocycl. Chem.* **1975**, *12*, 985−988.

(8) See for example: (a) Boulton, A. J.; Frank, F.; Huckstep, M. R. *Gazz. Chim. Ital.* **1982**, *112*, 181−183. (b) Sheremetev, A. B.; Makhova, N. N.; Friedrichsen, W. *Adv. Heterocycl. Chem.*, **2001**, *78*, 66−188. (c) Makhova, N. N.; Ovchinnikov, I. V.; Kulikov, A. S.; Molotov, S. I.; Baryshnikova, E. L. *Pure Appl. Chem.* **2004**, *76*, 1691−1703.

(9) The base catalysis increases the nucleophilic character of the ZH side-chain moiety. Nevertheless, the occurrence of an acid-catalyzed pathway has been recently observed for the BKR of *Z*-arylhydrazones of 3-benzoyl-5-amino-1,2,4-oxadiazole into 1,2,3-triazoles.[6b,c,e] Moreover, copper(II) acetate catalysis has been reported for the BKR of some arylhydrazones of 3-benzoyl-1-oxa-2-azoles. Buscemi, S.; Frenna, V.; Vivona, N.; Spinelli, D. *J. Chem. Soc., Perkin Trans. 1* **1993**, 2491−2493.

(10) (a) Vivona, N.; Frenna, V.; Buscemi, S.; Ruccia, M. *J. Heterocycl. Chem.* **1985**, *22*, 97−99. (b) Vivona, N.; Buscemi, S.; Frenna, V.; Ruccia, M.; Condò, M. *J. Chem. Res. (M)* **1985**, 2184−2197; (*S*) **1985**, 190. (c) Andrianov, V. G.; Eremeev, A. V. *Chem. Heterocycl. Compd. (Engl. Transl.)* **1990**, *26*, 1199−1213.

(11) Interestingly, the transformation of 1,2,5-oxadiazole-2-oxides into 1,2,4-oxadiazoles has been claimed as a first step along two cascade BKRs of 3-arylazo-4-acylaminofuroxans into 4-amino-5-nitro-2*H*-1,2,3-triazoles.[8c] See also: (a) Baryshnikova, E. L.; Kulikov, A. S.; Ovchinnikov, I. V.; Solomentsev, V. S.; Makhova, N. N. *Mendeleev Commun.* **2001**, 230−232. (b) Molotov, S. I.; Kulikov, A. S.; Strelenko, Yu. A.; Makhova, N. N.; Lyssenko, K. A. *Russ. Chem. Bull.* (*Engl. Transl.*) **2003**, *52*, 1829−1834.

(12) Harsani, K. *J. Heterocycl. Chem.* **1973**, *10*, 957−961.

(13) Kübel, B. *Monatsh. Chem.* **1983**, *114*, 373−376. For a similar rearrangement leading to a 5-trifluoromethylisoxazole, see: Sumimoto, S.; Ishizuka, I.; Ueda, S; Takase, A.; Okuno, K. Jpn. Patent 01009978, 1989; *Chem. Abstr.* **1989**, *111*, 57722.

(14) Buscemi, S.; Frenna, V.; Vivona, N. *Heterocycles* **1991**, *32*, 1765−1772.

(15) (a) Vivona, N.; Ruccia, M.; Cusmano, G.; Marino, M. L.; Spinelli, D. *J. Heterocycl. Chem.* **1975**, *12*, 1327−1328. (b) La Manna, G.; Buscemi, S.; Frenna, V.; Vivona, N.; Spinelli, D. *Heterocycles* **1991**, *32*, 1547−1557. (c) Andrianov, V. G.; Makushenkov, S. V.; Eremeev, A. V. *Mendeleev Commun.* **1992**, 129−130. (d) Buscemi, S.; Frenna, V.; Vivona, N.; Petrillo, G.; Spinelli, D. *Tetrahedron* **1995**, *51*, 5133−5142. (e) La Manna, G.; Buscemi, S.; Vivona, N. *J. Mol. Struct. (THEOCHEM)* **1998**, *452*, 67−74. (f) Buscemi, S.; Frenna, V.; Pace, A.; Vivona, N.; Cosimelli, B.; Spinelli, D. *Eur. J. Org. Chem.* **2002**, 1417−1423. (g) Buscemi, S.; Pace, A.; Frenna, V.; Vivona, N. *Heterocycles* **2002**, *57*, 811−823.

SCHEME 3. General Scheme and Examples of Ring-Degenerate BKR of 1,2,4-Oxadiazoles

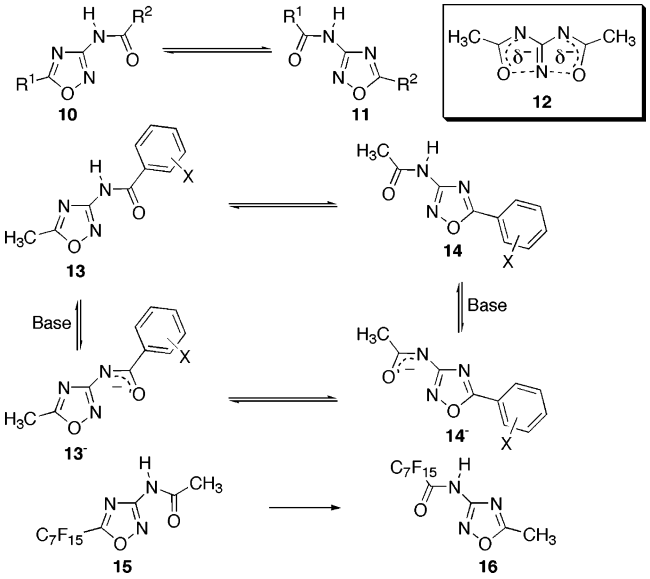

An interesting case is represented by 3-acylamino-1,2,4-oxadiazoles **10**, where the identity of the three-atom chains (A−B−D = X−Y−Z = N−C−O) allows a ring-degenerate BKR to occur (Scheme 3).[7,15,16]

A fully degenerate BKR has been evidenced[15a] in the case of the anion of the 3-acetylamino-5-methyl-1,2,4-oxadiazole (**10**; $R^1 = R^2 = CH_3$) for which the involvement of a planar symmetrical transition state **12** has been debated in several computational studies.[15b,c,e] For 3-aroylamino derivatives **13**, the substituents on the aryl moiety will differently affect the neutral (**13** ⇆ **14**) and anionic forms (**13**$^-$ ⇆ **14**$^-$) equilibria.[15d,f] When neutral forms are involved, the equilibrium is generally shifted toward the 5-aryl-substituted component **14** as a result of a diaryloid stabilization;[7,15d,f] by contrast, when anionic forms are considered, stabilization of the negative charge on the aroylamino chain plays an important role in the equilibrium.[15d,f] Interestingly, the electron-withdrawing ability of the perfluoroalkyl group determines an irreversible transformation of 3-acetylamino-5-perfluoroheptyl-1,2,4-oxadiazole **15** into the corresponding 3-perfluorooctanoylamino-1,2,4-oxadiazole **16**.[15g]

Besides the several examples of BKR, there are many other ring rearrangements in which the 1,2,4-oxadiazole system is involved. Among azoles, in fact, the 1,2,4-oxadiazole is one of the least aromatic[17] and easily undergoes photochemical[1,18] or ANRORC-like[19] rearrangements into more stable heterocycles.

In a recent paper, we investigated the competition between three different photoinduced rearrangements of 3-amino (or 3-alkylamino)-1,2,4-oxadiazoles (**17**; R = H, alkyl) and pointed out the importance of anionic forms and tautomeric equilibria in determining the experimentally observed reactivity.[1] The role of the photoirradiation was determinant to weaken the O−N bond and promote the formation of strained three-membered heterocyclic intermediates. One of the three rearrangements involved a C(3)−N(2) migration−nucleophilic attack−cyclization (MNAC) route, which was evidenced in the thermally driven reactivity of one of the proposed photolytic intermediates (Scheme 4a). For instance, in the case of **17** (R = alkyl), this reaction route implies the formation of a diazirine intermediate (**19**; R = alkyl) which can be interpreted as a one-atom side-chain rearrangement involving the exocyclic nitrogen.[1,20] The diazirine (**19**; R = alkyl) completes the C(3)−N(2) migration step by developing into the more stable carbodiimide (**20**; R = alkyl). The latter is attacked by an external nucleophile and finally cyclizes into the triazole (**22**; R = alkyl) (Scheme 4a).

Only a few examples of thermally induced MNAC reactivity are reported, all requiring the first atom of the side chain to be a strong nucleophilic site. One case regards the base-promoted rearrangement of 3-*N*-arylamino-5-methoxy-1,2,4-oxadiazoles into 1,2,4-triazolin-5-ones.[20a] In the case of enaminoketone **23** (Scheme 4b), the availability of an internal nucleophile in the carbodiimide **26** (arising from diazirine **25**) allows one to complete the nucleophilic attack and the cyclization in a single step producing the pyrazole **27**.[20b] Interestingly, a competing rearrangement into the imidazole **28**, through the carbanion **24**, is also observed[20b] following the classic three-atom (N−C−C) side-chain BKR.[21]

On the basis of these results, it is our opinion that, while photoinduced MNAC rearrangements follow a downhill path starting from neutral or anionic excited states, similar reactions in the ground state require (i) a strong base catalysis to create an anionic nucleophilic center at the first atom of the side chain, and (ii) heating to overcome the activation barrier for the formation of strained three-membered ring intermediates.

Because of the potential acidity of the N−H proton, 3-acylamino-1,2,4-oxadiazoles are suitable substrates to assess the

(16) Ring-degenerate rearrangements of O−N bond-containing azoles are also known in the 1,2,5-oxadiazole series.[10c] See also: (a) Andrianov, V. G.; Semenikhina, V. G.; Eremeev, A. V.; Gaukhman, A. P. *Chem. Heterocycl. Compd. (Engl. Transl.)* **1988**, *24*, 1410. (b) Andrianov, V. G.; Semenikhina, V. G.; Eremeev, A. V. *Chem. Heterocycl. Compd. (Engl. Transl.)* **1991**, *27*, 102−104.

(17) In the class of five-membered heterocyclic systems, 1,2,4-oxadiazoles are among the least aromatic with an index of aromaticity $I_5 = 39$ or $I_A = 48$. (a) Bird, C. V. *Tetrahedron* **1985**, *41*, 1409−1414. (b) Bird, C. V. *Tetrahedron* **1992**, *48*, 335−340.

(18) For photoinduced rearrangements involving the 1,2,4-oxadiazole heterocycle, see: (a) Vivona, N.; Buscemi, S. *Heterocycles* **1995**, *41*, 2095−2116 and references cited therein. (b) Buscemi, S.; Vivona, N.; Caronna, T. *J. Org. Chem.* **1995**, *60*, 4096−4101. (c) Buscemi, S.; Vivona, N.; Caronna, T. *J. Org. Chem.* **1996**, *61*, 8397−8401. (d) Vivona, N.; Buscemi, S.; Asta, S.; Caronna, T. *Tetrahedron* **1997**, *53*, 12629−12636. (e) Buscemi, S.; Pace, A.; Vivona, N.; Caronna, T.; Galia, A. *J. Org. Chem.* **1999**, *64*, 7028−7033. (f) Buscemi, S.; Pace, A.; Vivona, N.; Caronna, T. *J. Heterocycl. Chem.* **2001**, *38*, 777−780. (g) Buscemi, S.; Pace, A.; Pibiri, I.; Vivona, N. *J. Org. Chem.* **2002**, *67*, 6253−6255. (h) Buscemi, S.; D'Auria, M.; Pace, A.; Pibiri, I.; Vivona, N. *Tetrahedron* **2004**, *60*, 3243−3249. (i) Pace, A.; Pibiri, I.; Buscemi, S.; Vivona, N. *J. Org. Chem.* **2004**, *69*, 4108−4115. (j) Buscemi, S.; Pace, A.; Palumbo Piccionello, A.; Pibiri, I.; Vivona, N. *Heterocycles* **2004**, *63*, 1619−1628. (k) Pace, A.; Pibiri, I.; Buscemi, S.; Vivona, N. *Heterocycles* **2004**, *63*, 2627−2648. (l) Buscemi, S.; Pace, A.; Palumbo Piccionello, A.; Pibiri, I.; Vivona, N. *Heterocycles* **2005**, *65*, 387−394. (m) Pace, A.; Buscemi, S.; Vivona, N. *J. Org. Chem.* **2005**, *70*, 2322−2324.

(19) For recent examples of ANRORC[2d] (*Addition of a Nucleophile Ring-Opening Ring-Closure*) rearrangements of 1,2,4-oxadiazoles see: (a) Buscemi, S.; Pace, A.; Palumbo Piccionello, A.; Macaluso, G.; Vivona, N.; Spinelli, D.; Giorgi, G. *J. Org. Chem.* **2005**, *70*, 3288−3291. (b) Buscemi, S.; Pace, A.; Pibiri, I.; Vivona, N.; Spinelli, D. *J. Org. Chem.* **2003**, *68*, 605−608. (c) Buscemi, S.; Pace, A.; Pibiri, I.; Vivona, N.; Lanza, C. Z.; Spinelli, D. *Eur. J. Org. Chem.* **2004**, 974−980. (d) Buscemi, S.; Pace, A.; Palumbo Piccionello, A.; Pibiri, I.; Vivona, N.; Giorgi, G.; Mazzanti, A.; Spinelli, D. *J. Org. Chem.* **2006**, *71*, 8106−8113. (e) Palumbo Piccionello, A.; Pace, A.; Pibiri, I.; Buscemi, S.; Vivona, N. *Tetrahedron* **2006**, *62*, 8792−8797.

(20) (a) Jones, S. S.; Staiger, D. B.; Chodosh, D. F. *J. Org. Chem.* **1982**, *47*, 1969−1971. (b) Braun, M.; Buchi, G.; Bushey, D. F. *J. Am. Chem. Soc.* **1978**, *100*, 4208−4213.

(21) (a) Ruccia, M.; Vivona, N.; Cusmano, G. *Tetrahedron Lett.* **1972**, 4959−4960. (b) Ruccia, M.; Vivona, N.; Cusmano, G. *Tetrahedron* **1974**, *30*, 3859−3864.

SCHEME 4. Photochemically (a) and Thermally (b) Induced Examples of the C(3)−N(2) Migration−Nucleophilic Attack−Cyclization (MNAC) Rearrangements in 1,2,4-Oxadiazoles

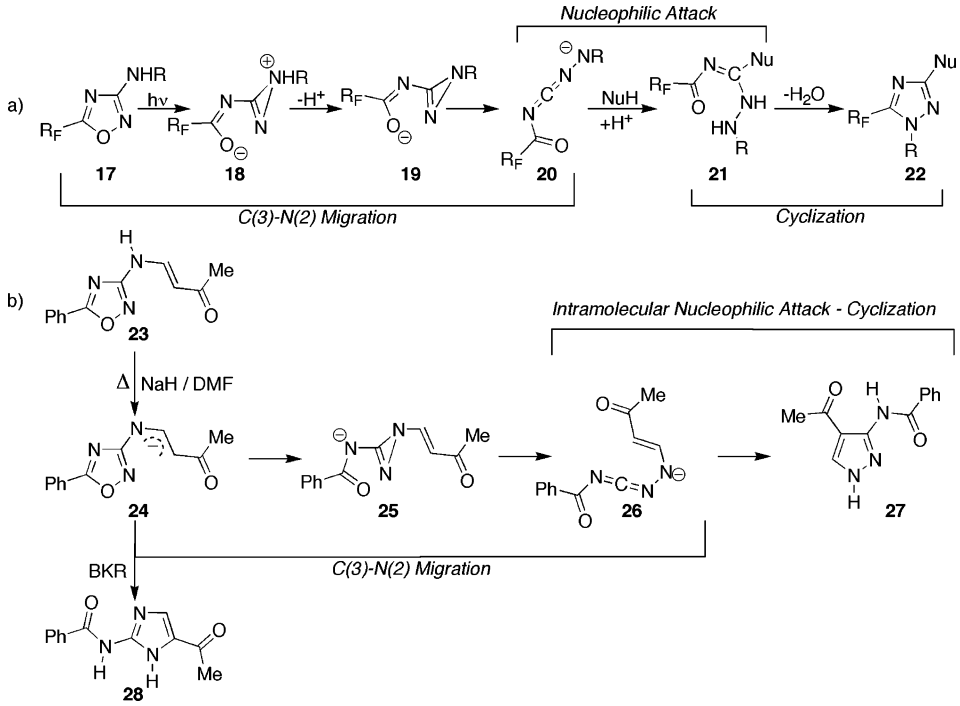

SCHEME 5. Base-Catalyzed Thermally Induced Rearrangements of 3-Acylamino-1,2,4-oxadiazoles

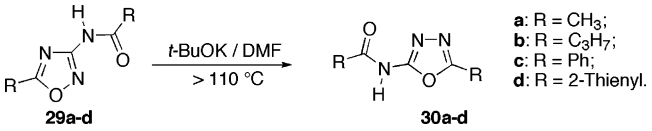

possibility of a thermally induced one-atom side-chain rearrangement to occur. As mentioned above (see Scheme 3), equilibria of these substrates have been studied considering different substituents. However, the anionic forms' equilibria have never been thoroughly investigated at a temperature higher than 40 °C,[22] and this might have precluded the observation of energetically higher reaction pathways.

In this article, we report on (i) a newly discovered thermally induced base-catalyzed rearrangement of 3-acylamino-1,2,4-oxadiazoles into 2-acylamino-1,3,4-oxadiazoles and (ii) a theoretical study, performed by DFT calculations, to rationalize the experimental findings and to determine the structures and the energies of intermediates and transition states involved in the proposed reaction pathways.

Results and Discussion

At first, we investigated the reactivity of 3-acylamino-1,2,4-oxadiazoles **29a**−**d**, whose fully degenerate BKR would be nonproductive, to assess the occurrence of a one-atom side-chain rearrangement. Oxadiazoles **29a**−**d**, heated in DMF at 150 °C and in the presence of *t*-BuOK, produced the corresponding 2-acylamino-1,3,4-oxadiazoles **30a**−**d** in 60−77% yields (Scheme 5).

The observed rearrangement must involve deprotonated intermediates since, in the absence of base and under the same conditions, the starting material remained essentially unchanged. For a comparison with previous investigations,[23] an analytical scale reaction of 3-acetylamino-5-methyl-1,2,4-oxadiazole **29a** was also performed in DMF-d_7 containing *t*-BuOK and followed by ^{1}H NMR as a function of temperature and reaction time (Figure 1). The NMR spectra showed coalescence of the two methyl signals of **29a**$^-$ at about 115 °C, in agreement with previously reported observations in DMSO-d_6.[15a] Moreover, by standing at temperatures higher than 110 °C, the formation of 1,3,4-oxadiazole **30a** is significantly observed, as a competitive reaction, together with the fast Boulton−Katritzky rearrangement (Figure 1). However, while the BKR is a reversible process, the transformation into 1,3,4-oxadiazole **30a** is irreversible. Finally, if cooled before completion of the reaction, the spectrum of the reaction mixture shows the presence of both 1,2,4-oxadiazole **29a**$^-$ and 1,3,4-oxadiazole **30a**$^-$.

The rearrangement into 1,3,4-oxadiazoles could be explained by two alternative, but experimentally indistinguishable, routes both involving a diazirine (**31** or **31′**) and a carbodiimide intermediate **32** (Scheme 6). In the MNAC route, the exocyclic nitrogen of the starting oxadiazole is involved in the formation of the diazirine intermediate **31**, causing the cleavage of the O−N ring bond. In the RCRE route, instead, the O−N bond is broken and the original N(4) of the oxadiazole ring is involved with the N(2) in the formation of the diazirine **31′**, chemically but not topologically identical to **31**. To determine the energetic relationship between the BKR, RCRE, and MNAC routes, we performed a computational study at the hybrid DFT B3LYP

(22) Higher temperatures were used for a short experimental time during a dynamic NMR study on the BKR of the anion of 3-acetylamino-5-methyl-1,2,4-oxadiazole **29a**.[15a]

(23) A previously reported,[15a] dynamic NMR experiment, performed in DMSO-d_6 on 3-acetylamino-5-methyl-1,2,4-oxadiazole **29a** in the presence of *t*-BuOK, showed coalescence of the two methyl signals at 112 °C, and an activation barrier of $\Delta G^{\ddagger} = 82 \pm 1.7$ kJ/mol was evaluated for the BKR equilibrium of chemically, but not topologically, identical **29a**$^-$ and **29a′**$^-$ anions (see Figure 2). However, in that occasion, due to the short time spent at 112 °C, the low resolution of NMR spectra, and the extended exchange of the methyl protons with DMSO deuteria, no further rearrangement was detected.

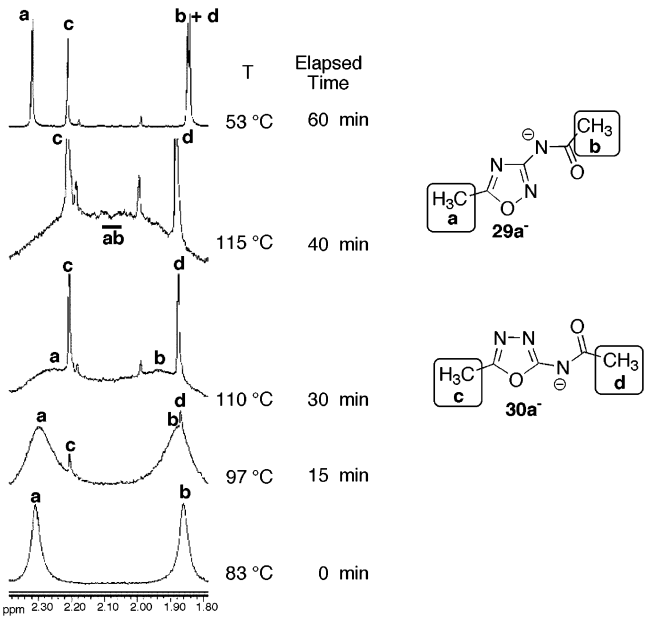

FIGURE 1. ^{1}H NMR spectra of compound **29a** in DMF-d_7 in the presence of *t*-BuOK as a function of temperature and reaction time.

level (see Computational Details in the Experimental Section), using 3-acetylamino-5-methyl-1,2,4-oxadiazole **29a** as a model compound, and the results obtained, both in vacuo and in the mimicked DMSO solvent,[24] are summarized in Table 1 and illustrated in Figure 2.

The energies calculated along the reaction coordinate of neutral and deprotonated **29a** and **29a**$^-$, and the geometries of the transition states and intermediates, allowed us to rationalize several aspects of this newly discovered reactivity of 3-acylamino-1,2,4-oxadiazoles. As expected, in agreement with the experimental results, the 1,3,4-oxadiazole product, in either its neutral **30a** or anionic **30a**$^-$ forms, is by far more stable than 1,2,4-oxadiazole **29a** or **29a**$^-$, respectively. Along the anionic reaction coordinate, the three routes available for the evolution of starting 1,2,4-oxadiazole **29a**$^-$ are energetically well differentiated. The fully degenerate Boulton−Katritzky rearrangement equilibrium, **29a**$^-$ ⇆ **29a′**$^-$, involves a fully planar transition state with C_{2v} symmetry and has the lowest activation energy ($\Delta G^{\ddagger}_{BKR}$ = 79.1 kJ/mol) among the competing reactions. The calculated value is in excellent agreement with the activation barrier, $\Delta G^{\ddagger} = 82 \pm 1.7$ kJ/mol, experimentally measured in a previous study,[15a] and made us confident about the quality of the chosen computational approach. Both the MNAC and the RCRE routes, instead, require an initial highly endoergonic step leading to a strained diazirine intermediate (**31** or **31′**). The high activation energy of the first step, **29a**$^-$ → **31**, of the MNAC route ($\Delta G^{\ddagger}_{MNAC}$ = 131.0 kJ/mol) can be justified considering the remarkable bending of the $N_{exocyclic}$−C(3)−N(2) bond angle which is required along this step. Moreover, a rotation of the C(3)−$N_{exocyclic}$ bond is required to allow the overlap between the $N_{exociclic}$ (nucleophilic site) and N(2) (electrophilic site) orbitals; this rotation drives the carbonyl group on a plane orthogonal to the rest of the molecule with consequent loss of conjugation. In this step, the cleavage of the O−N ring bond is anchimerically assisted by the attack of the $N_{exocyclic}$ moiety on the N(2). In the absence of such assistance, the cleavage of the O−N ring bond in the first step, **29a**$^-$ → **31′**, of the RCRE route requires overcoming an even higher activation barrier ($\Delta G^{\ddagger}_{RCRE}$ = 192.5 kJ/mol) and is therefore the less favored route.

Continuing along the reaction coordinate, the diazirine intermediate **31** can follow two alternative routes: (i) the equilibration, through a one-atom side-chain fully degenerate rearrangement, with the equivalent diazirine **31′**; this rearrangement involves a TS with C_2 symmetry and has an activation barrier of 88.9 kJ/mol,[25] which is of the same order of magnitude as those calculated for **29a**$^-$ → **31** and **29a**$^-$ ⇆ **29a′**$^-$ processes; (ii) the development into the more stable carbodiimide **32** which will eventually cyclize into the anionic 1,3,4-oxadiazole **30a**$^-$. This latter route implies an initial conformational change of diazirine **31** (or **31′**) into **31″**, less stable by 5.2 kJ/mol; from this conformer, the transformation into the carbodiimide **32** has an activation barrier of only 18.9 kJ/mol; therefore, this second route will be favored. The final step consists of a fast cyclization of intermediate **32** into the 1,3,4-oxadiazole product **30**$^-$. In summary, while the base-catalyzed BKR is a fast reversible equilibrium, the MNAC route is a slow irreversible reaction which requires higher temperatures to be initiated and to produce the more stable 1,3,4-oxadiazoles; finally, the RCRE is the less favored pathway in the competition.

This mechanistic picture has been further verified by studying the reactivity of differently substituted 3-acylamino-1,2,4-oxadiazoles **33** and **36** (Scheme 7). Each one of these isomers, heated in DMF/*t*-BuOK in two separate preparative scale experiments, yielded a mixture of 1,3,4-oxadiazoles isomers **34** and **35** in approximately the same ratio (**34**:**35** = 70:30).

First of all, it is worth remarking that starting 1,2,4-oxadiazoles **33** and **36** correlate with each other through a BKR equilibrium involving either neutral or anionic species.[7,15d] In this case, the equilibrium composition for the neutral BKR **33** ⇆ **36** did not significantly vary upon solvent change from MeOH (**33**:**36** = 91:9 at 40 °C)[15d] to DMSO or DMF (see Experimental Section). An anionic equilibrium composition of **33**$^-$:**36**$^-$ = 63:37 was determined at 40 °C using a *t*-BuOK/

(24) An analytical reaction performed on representative **29a** in DMSO/*t*-BuOK gave comparable results to those obtained in DMF. Therefore, although preparative scale reactions described in this article have been performed in DMF, we chose to use the available DMSO model solvent to mimic the polar aprotic solvent media in our computational study.

(25) In a previous paper,[1] we pointed out the possibility of a thermal equilibrium to occur between the diazirine **B** (formed through a migration step from oxadiazole **A**) and the diazirine **C** (originated through a ring-contraction step from oxadiazole **A**).

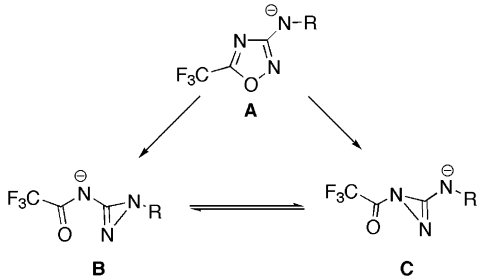

In that occasion, the occurrence of a **B** → **C** transformation, for R = H, was claimed to justify the experimental findings. As a comparison, the activation barriers for this diazirine interconversion in MeOH were calculated to be $\Delta G^{\ddagger}$ = 105.0 kJ/mol (for **B** → **C**; R = H), $\Delta G^{\ddagger}$ = 96.2 kJ/mol (for **C** → **B**; R = H), $\Delta G^{\ddagger}$ = 129.4 kJ/mol (for **B** → **C**; R = CH_3), and $\Delta G^{\ddagger}$ = 74.3 kJ/mol (for **C** → **B**; R = CH_3).

SCHEME 6. Alternative Reaction Routes for the Ring Rearrangement of 1,2,4-Oxadiazole 29a into 1,3,4-Oxadiazole 30a

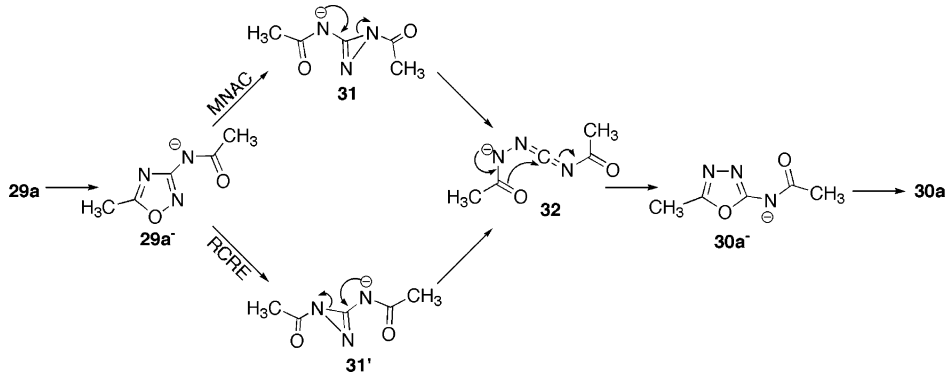

TABLE 1. Standard Free Energy Values (Δ*G*°, kJ/mol) Relative to 29a,[a] for Neutral, and to 29a⁻,[a] for Anionic Species or Transition States, and Activation Barriers (Δ*G*‡, kJ/mol), Relative to the Given Starting Compound, along the Anionic Reaction Coordinate, Calculated In Vacuo and in DMSO at 298.15 K

Neutral Species	Δ*G*° in vacuo	Δ*G*° in DMSO	Anionic Species	Δ*G*° in vacuo	Δ*G*° in DMSO
29a	0.0	0.0	**29a**⁻	0.0	0.0
30a	−20.7	−19.0	**30a**⁻	−48.3	−41.1
			31	73.1	104.2
			31″	70.6	109.4
			32	−11.2	29.2

Transition States	Δ*G*° in vacuo	Δ*G*° in DMSO	Δ*G*‡ in vacuo	Δ*G*‡ in DMSO
[**29a**⁻ → **29a′**⁻]‡	64.2	79.1	64.2	79.1
[**29a**⁻→**31**]‡	102.0	131.0	102.0	131.0
[**29a**⁻ → **31′**]‡	160.1	192.5	160.1	192.5
[**31** → **31′**]‡	152.7	193.1	79.6	88.9
[**31″** → **32**]‡	96.9	128.3	26.3	18.9
[**32** → **30a**⁻]‡	8.2	36.3	19.4	7.1

[a] The standard free energy values calculated at the B3LYP/6-31++G(d,p) level for compounds **29a** and for **29a**⁻ are −509.37138 and −508.82729 au, respectively; the solvation free energy values for **29a** and for **29a**⁻ are −7.60 and −55.83 kcal/mol, respectively (see Computational Details in the Experimental Section).

oxadiazole = 0.5 ratio in DMSO-d_6.[26] This result is in agreement with the previously reported ratio **33**⁻:**36**⁻ = 62:38 in CD_3OD at 40 °C, determined by using a base/substrate ratio of 1.5,[15d] and shows the little dependence from the solvent also for the anionic BKR equilibrium.

Besides undergoing the Boulton−Katritzky rearrangement, each anion (**33**⁻ or **36**⁻) of the starting 1,2,4-oxadiazoles is able to produce any of the 1,3,4-oxadiazoles isomers **34** and **35** through different competing pathways (Scheme 8). DFT calculations, performed on neutral and anionic species along the reaction coordinate of both 1,2,4-oxadiazoles **33** and **36**, clarified some aspects of the observed reactivity, and the results are summarized in Table 2 and illustrated in Figure 3.

Also in this case, analogously to what observed for **29a** and **30a**, 1,3,4-oxadiazoles **34** and **35** and their anions **34**⁻ and **35**⁻ were more stable than the starting 1,2,4-oxadiazoles **33** and **36** and their anions **33**⁻ and **36**⁻, respectively. Interestingly, the thermodynamic of structural change from 1,2,4-oxadiazole to 1,3,4-oxadiazole is not significantly affected by the change of the substituents (from methyl to phenyl) on either the amide chain or the oxadiazole ring. In fact, the free energy values of the 1,2,4-oxadiazole → 1,3,4-oxadiazole transformation $\Delta G^\circ_{1,3,4-1,2,4}$ are about −20 kJ/mol (for the neutral forms) and about −40 kJ/mol (for anionic forms) for compounds **29a**/**30a**, **33**/**35**, and **36**/**34** (see Tables 1 and 2).

By comparing values of Table 2, it is interesting to outline the considerable influence of the DMSO solvent in determining the relative stability especially of the anionic species involved in the process. In fact, for example, the stability order of anions **34**⁻ and **35**⁻ in DMSO is different than in vacuo. Another remarkable case is the energy difference between the anionic species **33**⁻ and **36**⁻. While in vacuo **33**⁻ is about 7 kJ/mol less stable than **36**⁻, in DMSO the difference decreases to 1.4 kJ/mol, and the two species can be considered as essentially isoenergetic, within the numerical accuracy of the selected computational method. This means that DMSO has a more pronounced stabilizing effect for **33**⁻ than for **36**⁻, in agreement with the experimentally established equilibrium composition in DMSO, **33**⁻:**36**⁻ = 63:37 (see above).[27] On the other hand, the stability order of neutral species is not affected by the solvent;

(26) An accurate determination of the anionic BKR equilibrium **33**⁻ ⇆ **36**⁻ composition would require a higher base/substrate ratio to guarantee for complete deprotonation of the starting oxadiazole.[15d] However, the use of *t*-BuOK/oxadiazole ratios higher than 0.5 in DMSO-d_6 was not achievable because of low solubility of the formed salts. Moreover, an even lower solubility of these salts was observed when DMF-d_7 was used.

(27) Calculations on anions **33**⁻ and **36**⁻ in MeOH showed anion **33**⁻ being 0.5 kJ/mol more stable than **36**⁻, in good agreement with the experimentally determined equilibrium composition in CD_3OD.[15d] On the other hand, due to the experimental difficulties encountered,[26] a rigorous comparison between the experimental and computational data is not possible in the case of BKR equilibrium **33**⁻ ⇆ **36**⁻ in DMSO for which the little discordance about the stability order is within the numerical accuracy of the computational method. In our opinion, only the explicit consideration of coordinating solvent molecules in our DFT calculation, in addition to the PCM approach, could in this isolated case reproduce the stability order, experimentally determined.

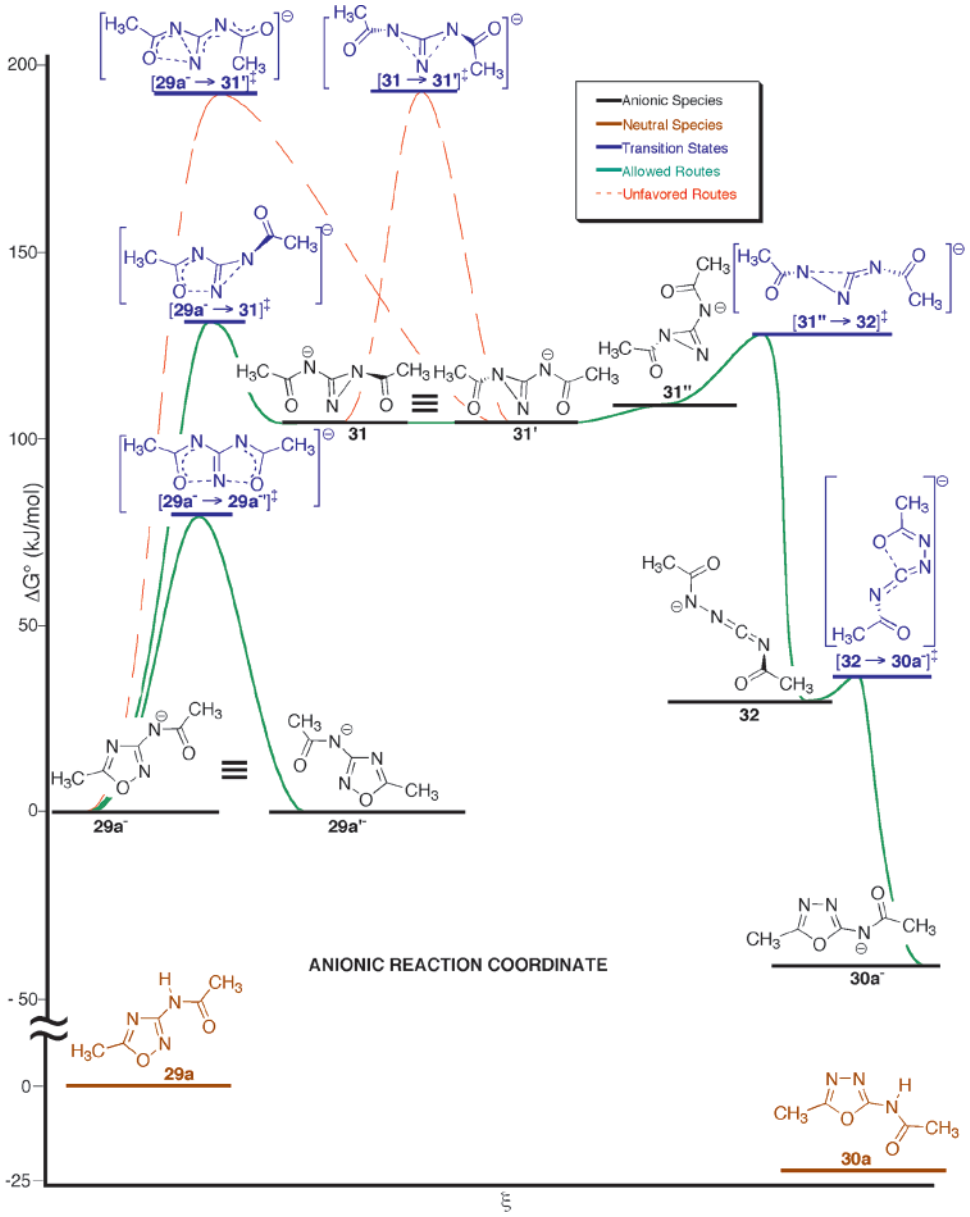

FIGURE 2. Standard free energy profiles along the reaction coordinate of 1,2,4-oxadiazole **29a** in solution, at 298.15 K.

SCHEME 7. Base-Catalyzed Thermal Rearrangements of 3-Acetylamino-5-phenyl- (33) and 3-Benzoylamino-5-methyl- (36) 1,2,4-oxadiazoles

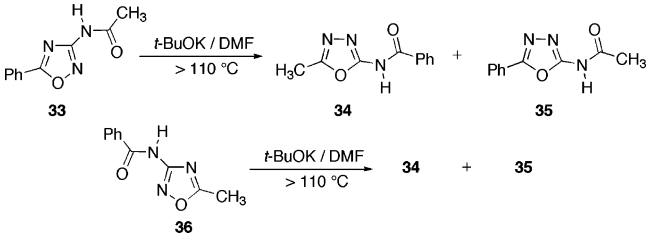

for instance, neutral oxadiazoles **33** is 7.9 kJ/mol more stable than **36** both in vacuo and in DMSO. These data are in agreement with the experimentally observed neutral BKR equilibrium significantly shifted in favor of **33** (**33**:**36** = 91.6:8.4 at 25 °C).

The calculated activation barrier for the Boulton−Katritzky rearrangement between anions **33**$^-$ and **36**$^-$ in DMSO ($\Delta G^{\ddagger}$ = 79.0 kJ/mol) is practically identical to the one calculated for the BKR of **29a**$^-$. Therefore, under the used reaction conditions (excess of *t*-BuOK and 150 °C), either oxadiazole **33** or **36** should undergo a fast BKR equilibrium yielding the anionic mixture **33**$^-$/**36**$^-$. From this equilibrium mixture, each of the oxadiazole anions, **33**$^-$ or **36**$^-$, can then follow either the RCRE or the MNAC route. The activation barriers for the RCRE route (**33**$^-$ → **39** or **36**$^-$ → **37**), respectively, 196 and 214 kJ/mol, are different along the two reaction coordinates of **33**$^-$ and **36**$^-$, resulting about 19 kJ/mol more favored in the case of **33**$^-$. On the other hand, the MNAC route (**33**$^-$ → **37** or **36**$^-$ → **39**) has a much lower activation energy, about 130 kJ/mol, which is almost identical for **33**$^-$ and **36**$^-$, and should be by far a more favored pathway than the RCRE.

In analogy with the study performed on the rearrangement of oxadiazole **29a**, we also considered the possible equilibration between the two diazirine intermediates **37** and **39**. Although involving a noteworthy activation barrier (80.5 kJ/mol), this equilibrium cannot be excluded on the basis of computational

SCHEME 8. Competition between BKR, MNAC, and RCRE Routes in the Rearrangements of Oxadiazoles 33 and 36

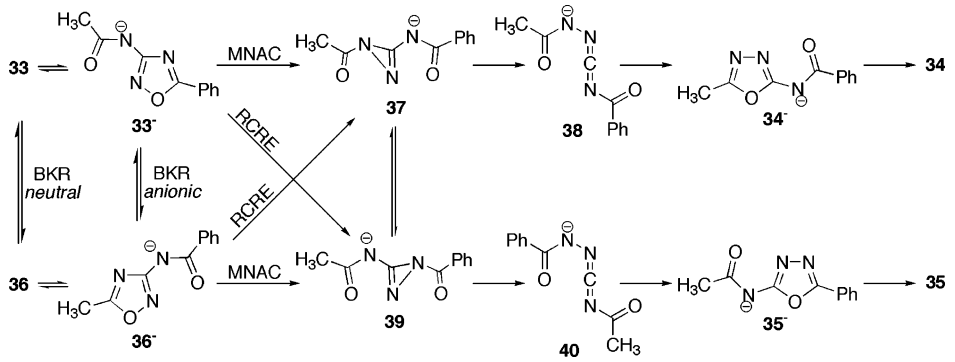

TABLE 2. Standard Free Energy Values (Δ*G*°, kJ/mol) Relative to 36,[a] for Neutral, and to 36⁻,[a] for Anionic Species or Transition States, and Activation Barriers (Δ*G*‡, kJ/mol), Relative to the Given Starting Compound, along the Anionic Reaction Coordinate, Calculated In Vacuo and in DMSO at 298.15 K

Neutral Species	Δ*G*° in vacuo	Δ*G*° in DMSO	Anionic Species	Δ*G*° in vacuo	Δ*G*° in DMSO
33	−7.9	−7.9	**33**⁻	6.7	1.4
34	−20.7	−18.2	**34**⁻	−44.9	−38.8
35	−30.7	−26.5	**35**⁻	−50.1	−37.1
36	0.0	0.0	**36**⁻	0.0	0.0
			37	81.7	107.9
			37′	77.9	111.5
			38	−1.5	34.2
			39	87.4	114.8
			39′	90.0	124.8
			40	−6.4	29.8

Transition States	Δ*G*° in vacuo	Δ*G*° in DMSO	Δ*G*‡ in vacuo	Δ*G*‡ in DMSO
[**33**⁻ → **36**⁻]‡	69.6	80.4	62.9	79.0
[**33**⁻ → **37**]‡	110.3	133.5	103.6	132.1
[**33**⁻ → **39**]‡	170.1	197.0	163.4	195.6
[**36**⁻ → **37**]‡	185.6	214.3	185.6	214.3
[**36**⁻ → **39**]‡	111.7	133.5	111.7	133.5
[**37** → **39**]‡	162.2	195.3	80.5	87.4
[**37′** → **38**]‡	106.9	129.7	29.0	18.2
[**39′** → **40**]‡	107.0	135.0	17.0	10.2
[**38** → **34**⁻]‡	17.2	39.0	18.7	4.8
[**40** → **35**⁻]‡	13.0	38.0	19.4	8.2

[a] The standard free energy values calculated at the B3LYP/6-31++G(d,p) level for compounds **36** and **36**⁻ are −701.06922 and −700.53489 au, respectively; the solvation free energy values for **36** and for **36**⁻ are −8.39 and −53.23 kcal/mol, respectively (see Computational Details in the Experimental Section).

kinetic data. In fact, such a barrier is of the same order of magnitude of the BKR barrier and is even lower than those calculated for the migration steps **33**⁻ → **37** and **36**⁻ → **39**; hence the **37** ⇆ **39** equilibrium should be accessible at the experimental temperatures and conditions. However, once a diazirine is formed, its evolution into the corresponding carbodiimide (**37** → **37′** → **38** or **39** → **39′** → **40**) has a much lower activation energy (10−20 kJ/mol) than its equilibration with the other diazirine.

Overall, the energy profiles along the reaction coordinate of the two oxadiazoles **33**⁻ and **36**⁻ are very similar; therefore, following the two irreversible MNAC routes, the transformation of **33**⁻ and **36**⁻ should occur at the same rate without provoking any significant shift of the fast (under the reaction conditions) reversible BKR equilibrium. This hypothesis is supported by the analytical NMR determinations, where the same product distribution of **34**⁻:**35**⁻ = 72:28 was obtained after heating, in two separate experiments, either oxadiazole **33** or **36** with 2 equiv of *t*-BuOK for 3 h at 150 °C in DMF-d_7 (see Experimental Section). Indeed, this product distribution resembles the BKR equilibrium composition **33**⁻:**36**⁻ = 63:37 observed at 40 °C in DMSO-d_6 (see above). Unfortunately, a rigorous comparison, under the same conditions, between the 1,3,4-oxadiazole final product distribution and the 1,2,4-oxadiazoles BKR equilibrium composition could not be achieved because of experimental difficulties.[26]

Finally, one may consider that, in the experimental conditions of the present study, the final 1,3,4-oxadiazoles' distribution is a function of their anion stability and is essentially thermodynamically, and not kinetically, controlled; in fact, in DMSO, **34**⁻ is 1.7 kJ/mol more stable than **35**⁻, which implies a theoretical **34**⁻:**35**⁻ = 62:38 ratio at 150 °C, in agreement with the experimentally observed product ratio.

Conclusions

The competition between two thermally induced rearrangements of 3-acylamino-1,2,4-oxadiazoles in the presence of *t*-BuOK has been rationalized in terms of process reversibility and reaction rates. The reversible ring-degenerate Boulton−Katritzky rearrangement is in competition with a slower, but irreversible, one-atom side-chain rearrangement leading to the more stable 1,3,4-oxadiazoles. This competition originates from the presence of two alternative nucleophilic sites in the side

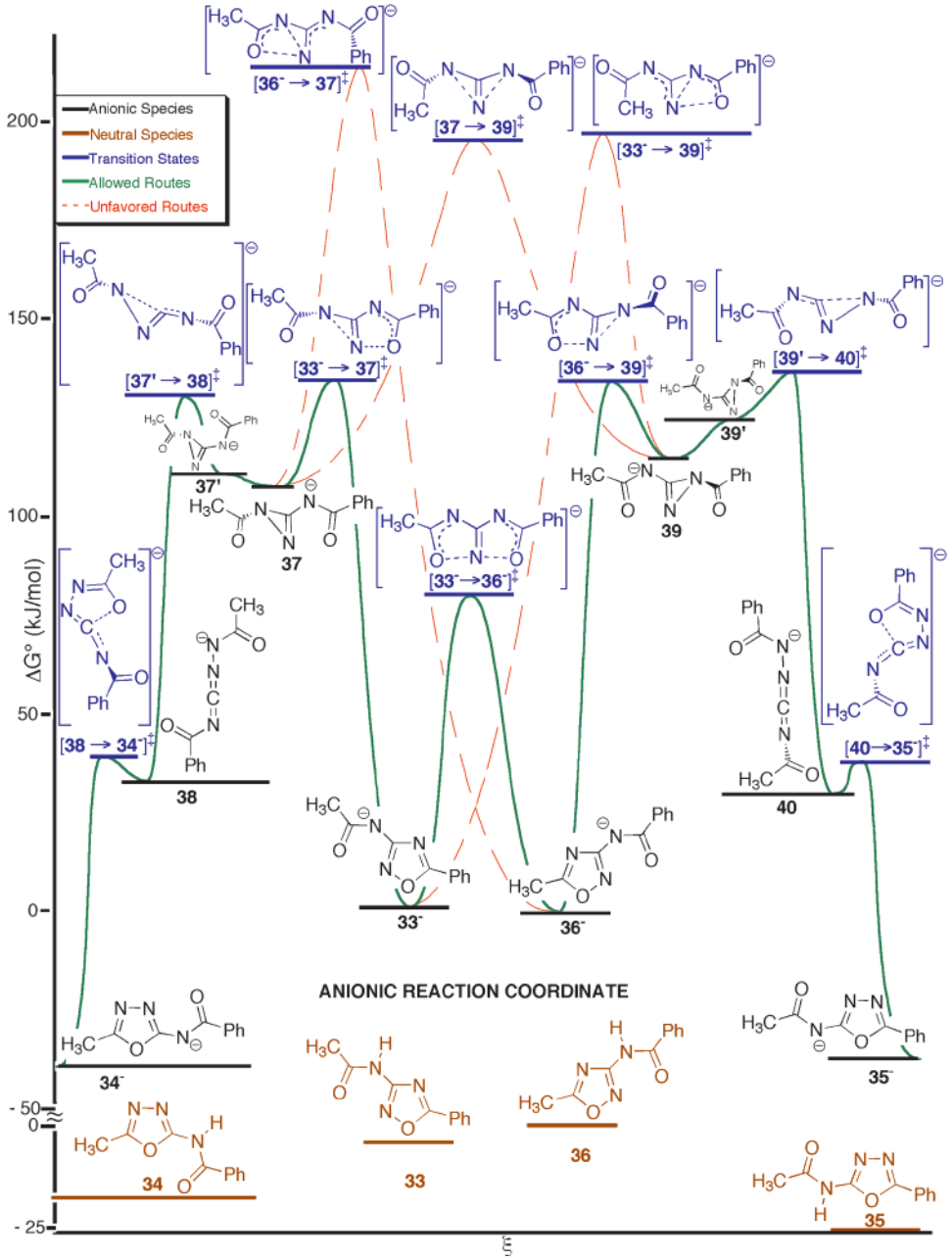

FIGURE 3. Standard free energy profiles along the reaction coordinate of 1,2,4-oxadiazoles **33** and **36** in solution, at 298.15 K.

chain of the deprotonated 3-acylamino-1,2,4-oxadiazole reagent. At a first glance, the anionic reagent can follow three possible routes each characterized by well differentiated transition states and activation energies. In the BKR, the nucleophilic attack of the side-chain oxygen atom on the electrophilic N(2) ring atom is geometrically favored and occurs through a planar [3.3.0] bicyclic transition state. In the migration step of the MNAC route, instead, the side-chain nitrogen atom is involved as a nucleophile in the formation of a planar [3.1.0] bicyclic transition state. This step requires higher temperatures to overcome the activation barrier mostly due to geometrical restrains. On the other hand, the planar [2.1.0] bicyclic transition state, involved in the ring-contraction step of the RCRE route, is too high in energy to be reached at the used reaction temperatures.

In a second time, the migration step of the MNAC route is then completed by the development of the diazirine into the more stable carbodiimide intermediate. This process is faster than the equilibration between the diazirine intermediates which, in turn, has an energy barrier comparable to that of the BKR and requires a planar [1.1.0] bicyclic transition state. Finally, since the carbodiimide intermediate possesses a nucleophilic site, an intramolecular nucleophilic attack occurs on the central carbodiimide carbon completing the nucleophilic attack−cyclization of the MNAC route in one step and yielding the final 1,3,4-oxadiazole product.

Overall, the driving force of the reaction is the higher stability of the 1,3,4-oxadiazole system with respect to the 1,2,4-oxadiazole heterocycle. The well different activation energies involved in the competing routes allow one to selectively control

which reaction will be observed, among the BKR and the MNAC route, by choosing the appropriate reaction temperature.

Experimental Section

Starting Materials. Compounds **29a**,[15a] **29c**,[28] **33**,[7] and **36** were synthesized as previously reported. Compounds **29b** and **29d** were similarly prepared by acylation of the corresponding 3-amino compounds,[15g] with the appropriate acyl chloride in pyridine at room temperature. 3-Butanoylamino-5-propyl-1,2,4-oxadiazole **29b** (83%) had mp 85−87 °C (from benzene/light petroleum). IR (nujol) 3250, 3229, 3107, 1699 cm^{-1}. ^1H NMR (300 MHz, DMSO-d_6): δ 0.94 (t, 3H, J = 7.4 Hz), 1.0 (t, 3H, J = 7.4 Hz), 1.64 (m, 2H), 1.79 (m, 2H), 2.40 (t, 2H, J = 7.2 Hz), 2.89 (t, 2H, J = 7.3 Hz), 11.02 (s, 1H). HRMS calcd for $C_9H_{15}N_3O_2$ 197.1164; found 197.1164. 3-(2-Thiophenecarbonyl)amino-5-(thien-2-yl)-1,2,4-oxadiazole **29d** (80%) had mp 188−190 °C (from benzene). IR (nujol) 3200, 3100, 1673 cm^{-1}. ^1H NMR (300 MHz, DMSO-d_6): 7.31 (dd, 1H, J = 4.6 Hz, J = 3.6 Hz), 7.43 (dd, 1H, J = 3.6 Hz, J = 4.2 Hz), 8.03 (d, 1H, J = 4.6 Hz), 8.08 (d, 1H, J = 3.6 Hz), 8.17 (d, 1H, J = 4.2 Hz), 8.26 (d, 1H, J = 3.6 Hz), 11.80 (s, 1H). HRMS calcd for $C_{11}H_7N_3O_2S_2$ 276.9980; found 276.9977.

General Procedure for Preparative Scale Base-Catalyzed Rearrangements of 3-Acylamino-1,2,4-oxadiazoles 29a-d, 33, and 36. 3-Acylamino-1,2,4-oxadiazoles **29a**−**d**, **33**, or **36** (300 mg) were dissolved in 5 mL of dry DMF together with 2.1 equiv of *t*-BuOK, and the mixture was allowed to stir at 150 °C for 6−8 h, until complete conversion of the starting substrate was reached. The reaction was quenched by addition of water and neutralized with concentrated HCl. The aqueous phase was then extracted with EtOAc (3 × 20 mL), and the combined organic layers were washed with H_2O, dried on Na_2SO_4, and filtered. After solvent removal, the residue was chromatographed using silica gel (0.040−0.063 mm) and mixtures of EtOAc and light petroleum (fraction boiling in the range 40−60 °C) in various ratios.

Rearrangement of 29a. Chromatography of the residue yielded 2-acetylamino-5-methyl-1,3,4-oxadiazole **30a** (0.18 g; 60%), mp 180−182 °C (from EtOH) (lit.[29] mp 180−181 °C). IR (nujol) 3148, 1736, 1725 cm^{-1}. ^1H NMR (300 MHz, DMSO-d_6): δ 2.17 (s, 3H), 2.49 (s, 3H), 11.44 (s, 1H).

Rearrangement of 29b. Chromatography of the residue yielded 2-butanoylamino-5-propyl-1,3,4-oxadiazole **30b** (0.23 g; 77%), mp 89−92 °C (from benzene/light petroleum). IR (nujol) 3150, 1708 cm^{-1}. ^1H NMR (300 MHz, DMSO-d_6): δ 0.95 (t, 3H, J = 7.3 Hz), 1.0 (t, 3H, J = 7.4 Hz) 1.63 (m, 2H), 1.74 (m, 2H), 2.42 (t, 2H, J = 7.3 Hz), 2.81 (t, 2H, J = 7.3 Hz), 11.48 (s, 1H). HRMS calcd for $C_9H_{15}N_3O_2$ 197.1164; found 197.1162.

Rearrangement of 29c. Chromatography of the residue yielded 2-benzoylamino-5-phenyl-1,3,4-oxadiazole **30c** (0.23 g; 77%), mp 205−206 °C (from MeOH) (lit.[29] mp 201−202 °C). IR (nujol) 3150, 1716 cm^{-1}. ^1H NMR (250 MHz, DMSO-d_6): δ 7.58−7.74 (m, 6H), 7.98−8.11 (m, 4H), 12.30 (s, 1H).

Rearrangement of 29d. Chromatography of the residue yielded 2-(2-thiophenecarbonyl)amino-5-(thien-2-yl)-1,3,4-oxadiazole **30d** (0.19 g; 63%), mp 210−212 °C (from EtOH). IR (nujol) 3107, 1700 cm^{-1}. ^1H NMR (300 MHz, DMSO-d_6): δ 7.30 (dd, 1H, J = 3.5 Hz, J = 4.7 Hz), 7.35 (dd, 1H, J = 4.7 Hz, J = 3.8 Hz), 7.81 (d, 1H, J = 3.8 Hz), 7.98 (d, 1H, J = 4.7 Hz), 8.01 (d, 1H, J = 4.7 Hz), 8.13 (d, 1H, J = 3.5 Hz), 12.44 (s, 1H). HRMS calcd for $C_{11}H_7N_3O_2S_2$ 276.9980; found 276.9976.

Rearrangement of 33. Chromatography of the residue yielded 0.26 g (87%) of a mixture of 1,3,4-oxadiazoles isomers **34** and **35** in a **34**:**35** = 70:30 ratio, determined by comparing integrals of the methyl ^1H NMR signals (in DMSO-d_6) of **34** (at δ = 2.56) and **35** (at δ = 2.23). Analytical samples of oxadiazoles **34** and **35** (obtained from enriched chromatographic fractions) were compared with authentic synthetic samples of **34** and **35**. 2-Benzoylamino-5-methyl-1,3,4-oxadiazole **34** had mp 184−186 °C (from EtOH). IR (nujol) 3122, 1714 cm^{-1}. ^1H NMR (300 MHz, DMSO-d_6): δ 2.56 (s, 3H), 7.65 (m, 3H), 8,00 (m, 2H), 12.04 (s, 1H). HRMS calcd for $C_{10}H_9N_3O_2$ 203.0695; found 203.0691. 2-Acetylamino-5-phenyl-1,3,4-oxadiazole **35** had mp 220−222 °C (from EtOH) (lit.[30] mp 223 °C). IR (nujol) 3136, 1729 cm^{-1}. ^1H NMR (300 MHz, DMSO-d_6): δ 2.23 (s, 3H), 7.66 (m, 3H), 7.97 (m, 2H), 11.77 (s, 1H).

TABLE 3. Equilibrium Composition of the BKR of Compounds 33 or 36 in Neutral Conditions

	DMSO-d_6		DMF-d_7	
temp (°C)	**33** (%)	**36** (%)	**33** (%)	**36** (%)
25	91.6	8.4	91.5	8.5
40	90.8	9.2	90.2	9.8
120	85.7	14.3	84.1	15.9

Rearrangement of 36. Chromatography of the residue yielded 0.27 g (90%) of a mixture of 1,3,4-oxadiazoles isomers **34** and **35** in a **34**:**35** = 68:32 ratio (determined by NMR as described above).

Dynamic NMR Experiment for the Rearrangement of 29a$^-$ in DMF. 1,2,4-Oxadiazole **29a** (6.0 mg; 0.04 mmol) was dissolved in DMF-d_7 (0.35 mL) and added to a solution of *t*-BuOK (7.0 mg; 0.06 mmol) in DMF-d_7 (0.4 mL) in an NMR tube. ^1H NMR spectra were registered on the same sample at different temperatures over a period of 60 min. Compound **29a**: ^1H NMR (300 MHz, DMF-d_7) δ 2.18 (s, 3H), 2.55 (s, 3H), 10.89 (s, 1H). Anion **29a**$^-$: ^1H NMR (300 MHz, DMF-d_7) δ 1.84 (s, 3H), 2.29 (s, 3H). Compound **30a**: ^1H NMR (300 MHz, DMF-d_7) δ 2.20 (s, 3H), 2.46 (s, 3H), 11.51 (s, 1H). Anion **30a**$^-$: ^1H NMR (300 MHz, DMF-d_7) δ 1.86 (s, 3H), 2.22 (s, 3H). Representative spectra are illustrated in Figure 1 in the chemical shift range of the methyl signals.

Equilibration between 33 and 36 in DMSO-d_6 and DMF-d_7. In four separate NMR tubes, either 3-acetylamino-5-phenyl-1,2,4-oxadiazole **33** (10.0 mg; 0.05 mmol) or 3-benzoylamino-5-methyl-1,2,4-oxadiazole **36** (10.0 mg; 0.05 mmol) was dissolved in DMSO-d_6 (0.75 mL) or DMF-d_7 (0.75 mL). The four tubes were kept under identical temperature conditions in a thermostated bath.

The composition of the **33**/**36** mixture (see Table 3) was determined by ^1H NMR, by comparison of the integrals of methyl signals of **33** (2.19 ppm in DMSO-d_6; 2.25 ppm in DMF-d_7) and **36** (2.64 ppm in DMSO-d_6; 2.61 ppm in DMF-d_7). The equilibrium was considered reached when the composition of the **33**/**36** mixtures, from either **33** or **36**, resulted the same.

Equilibration between 33 and 36 in DMSO-d_6 in the Presence of *t*-BuOK. In two separate NMR tubes, either **33** (6.0 mg; 0.03 mmol) or **36** (6.0 mg; 0.03 mmol) was dissolved in DMSO-d_6 (0.35 mL). A solution of *t*-BuOK (1.7 mg; 0.015 mmol) in DMSO-d_6 (0.4 mL) was added to each tube. The obtained solution, opaque at rt, became clear at 40 °C. Both tubes were kept in a thermostated bath at 40 °C for 2.5 h. The composition of the **33**$^-$/**36**$^-$ mixture was determined by ^1H NMR, by comparison of the integrals of methyl signals at 2.17 ppm (for **33**$^-$) and 2.43 ppm (for **36**$^-$). The obtained ratios were **33**$^-$:**36**$^-$ = 63.6:36.4 from **33**, and **33**$^-$:**36**$^-$ = 62.5:37.5 from **36**, indicating that the equilibrium was complete, within experimental error.

Analytical Determination of Product Distribution from Rearrangements of 33 and 36 in DMF-d_7 in the Presence of *t*-BuOK. In two separate NMR tubes, either **33** (4.0 mg; 0.02 mmol) or **36** (4.0 mg; 0.02 mmol) was dissolved in DMF-d_7 (0.35 mL). A solution of *t*-BuOK (4.5 mg; 0.04 mmol) in DMF-d_7 (0.4 mL) was added to each tube, and a precipitate of the potassium salts of **33**$^-$ and **36**$^-$ was formed. The two tubes were then kept in a thermostated bath for 3 h at 150 °C (temperature at which the suspension became a clear solution). After cooling at rt (no

(28) Buscemi, S.; Vivona, N. *Heterocycles* **1994**, *38*, 2423−2432.
(29) Hagedorn, I.; Winkelmann, H. D. *Chem. Ber.* **1966**, *99*, 850.
(30) Werber, G.; Maggio, F. *Ann. Chim. (Rome)* **1962**, *52*, 747−755.

precipitate was observed from the two pale-yellow solutions), the composition of the $\mathbf{34}^-/\mathbf{35}^-$ mixture was determined by ^{1}H NMR, by comparison of the integrals of methyl signals at 2.28 ppm (for $\mathbf{34}^-$) and 1.91 ppm (for $\mathbf{35}^-$). The obtained ratios, considered equal within experimental error, were $\mathbf{34}^-:\mathbf{35}^- = 71.7:28.3$ from **33**, and $\mathbf{34}^-:\mathbf{35}^- = 72.2:27.8$ from **36**.

Computational Details. The molecular and anionic species considered, shown in Figures 2 and 3, were the lowest energy tautomers and/or conformers found for each isomer in the DMSO solvent (see below). Their geometry was fully optimized by using the hybrid DFT B3LYP method[31] and the 6-31++G(d,p) basis set.[32] Their Cartesian coordinates are available in the Supporting Information.

Transition-state structures were found by the synchronous transit guided quasi-Newton method.[33] Vibration frequency calculations, within the harmonic approximation, were performed to confirm whether each obtained geometry represented a transition state or a minimum in the potential energy surface. All of the minimum energy structures presented only real vibrational frequencies, whereas all of the transition state structures found were first-order saddle points.

To take into account the relative stabilization of intermediates, the standard free energies, at 298.15 K, of the considered species have been evaluated by vibrational frequency calculations of the in vacuo species. Their free energy in DMSO solution was evaluated by adding the solvation free energy to the free energy of the species in vacuo.[34] The solvation free energy in DMSO was calculated by the conductor-like polarized continuum model,[35] without further optimization of the geometry (i.e., single point calculations) within the solvent medium. Some test cases have in fact demonstrated that the subsequent geometry optimization in DMSO, although computationally expensive, did not produce significant differences with the structures and the solvation free energies evaluated for the geometries already optimized in vacuo.

All calculations were performed by the Gaussian98 program package.[36]

Acknowledgment. Financial support from the University of Palermo is gratefully acknowledged.

Supporting Information Available: Cartesian coordinates, B3LYP energy (in au), and standard thermochemical data (in au) at 298.15 K of all compounds and transition states reported in Tables 1 and 2 as well as illustrated in Figures 2 and 3. ^{1}H NMR spectra of compounds **29b,d**, **30a−d**, **34**, and **35** in DMSO-d_6. This material is available free of charge via the Internet at http://pubs.acs.org.

JO701306T

(31) Becke, A. D. *J. Chem. Phys.* **1993**, *98*, 5648−5652.

(32) (a) Hehre, W. J.; Ditchfield, R.; Pople, J. A. *J. Chem. Phys.* **1972**, *56*, 2257−2261. (b) Clark, T.; Chandrasekhar, J.; Schleyer, P. V. R. *J. Comput. Chem.* **1983**, *4*, 294−301. (c) Krishnam, R.; Binkley, J. S.; Seeger, R.; Pople, J. A. *J. Chem. Phys.* **1980**, *72*, 650−654. (d) Gill, P. M. W.; Johnson, B. G.; Pople, J. A.; Frisch, M. J. *Chem. Phys. Lett.* **1992**, *197*, 499−505.

(33) Peng, C.; Schlegel, H. B. *Isr. J. Chem.* **1994**, *33*, 449−454.

(34) Cramer, C. J. *Essentials of Computational Chemistry*, 2nd ed.; Wiley: New York, 2004.

(35) Barone, V.; Cossi, M. *J. Phys. Chem. A* **1998**, *102*, 1995−2001.

(36) Frisch, M. J.; Trucks, G. W.; Schlegel, H. B.; Scuseria, G. E.; Robb, M. A.; Cheeseman, J. R.; Zakrzewski, V. G.; Montgomery, J. A., Jr.; Stratmann, R. E.; Burant, J. C.; Dapprich, S.; Millam, J. M.; Daniels, A. D.; Kudin, K. N.; Strain, M. C.; Farkas, O.; Tomasi, J.; Barone, V.; Cossi, M.; Cammi, R.; Mennucci, B.; Pomelli, C.; Adamo, C.; Clifford, S.; Ochterski, J.; Petersson, G. A.; Ayala, P. Y.; Cui, Q.; Morokuma, K.; Malick, D. K.; Rabuck, A. D.; Raghavachari, K.; Foresman, J. B.; Cioslowski, J.; Ortiz, J. V.; Baboul, A. G.; Stefanov, B. B.; Liu, G.; Liashenko, A.; Piskorz, P.; Komaromi, I.; Gomperts, R.; Martin, R. L.; Fox, D. J.; Keith, T.; Al-Laham, M. A.; Peng, C. Y.; Nanayakkara, A.; Challacombe, M.; Gill, P. M. W.; Johnson, B.; Chen, W.; Wong, M. W.; Andres, J. L.; Gonzalez, C.; Head-Gordon, M.; Replogle, E. S.; Pople, J. A. *Gaussian 98*, revision A.8; Gaussian, Inc.: Pittsburgh, PA, 1998.